AIR ENTRAPMENT AND RESIDUAL STRESSES IN ROLLS WOUND WITH A RIDER ROLL

by

J. K. Good and S. M. Covell

Oklahoma State University
Stillwater, Oklahoma

ABSTRACT

Air is entrained during the process of winding webs. Rider rolls are often employed in an effort to reduce the amount of air which enters the wound roll. This paper presents the results of an experiment which allows the entrained air to be measured. With knowledge of the levels of entrapped air an algorithm was chosen to predict the amount of entrained air for various operating conditions. Finally the air entrapment algorithm was incorporated into a wound roll model such that the effect of the entrained air on the residual pressures within the wound roll could be studied.

NOMENCLATURE

d_{nip}	nip diameter
d_r	winding roll diameter
E_{nip}	Young's modulus of the nip
E_r	Young's modulus of the wound roll, radial direction
E'	$\dfrac{2}{\dfrac{1-\nu_{nip}^2}{E_{nip}}+\dfrac{1-\nu_r^2}{E_r}}$, equivalent (combined) modulus
E_t	in-plane modulus of web in the machine direction
F	nip load
h_o	minimum air film thickness
k	ellipticity contact parameter, typically ≥ 10 in rectangular contact elastohydrodynamic problems, dimensionless
L	nip load per unit width

P_{atm}	atmospheric pressure
p_{avg}	average pressure in the zone of contact
p_{max}	peak pressure in the zone of contact
P_o	pressure beneath the outer layer of the winding roll, T/s
r_e, R_x	$\frac{1}{1/s + 1/r_{nip}}$, equivalent (combined) radius
r_{nip}	nip radius
Ra	average web surface roughness
s	outer radius of winding roll
T	web tension per unit width
T_w	web line stress
U	$\frac{\eta V}{E' R_x}$, velocity parameter, dimensionless
V	web line velocity
W	$\frac{F}{E' R_x^2}$, nip load parameter, dimensionless
η	dynamic viscosity of air, $3.077*10^{-7}$ N-min/m^2 @ 27^{o}C
μ	coefficient of friction
σ	web surface roughness, r.m.s.
σ_r	radial pressure in wound roll
ν_{nip}	Poisson's ratio for the nip or rider roll
ν_r	Poisson's ratio for the wound roll

INTRODUCTION

Air entrapment has historically been both a bane and blessing in the winding of webs. Entrapped air results in softer wound rolls which have lower radial stresses. The entrapped air may be beneficial to prevent blocking of the web surfaces or possibly to prevent yielding of the web during viscoelastic recovery. The entrapped air may also be detrimental to roll quality. Lateral web shear almost always exists due to misalignment of web machinery or to nonuniformity of the web. When the entrained air layer becomes comparable to the combined roughness of the contacting web surfaces, the available interlayer traction becomes minimal as the traction capacity becomes controlled by the viscosity of air as the layers separate. Given web shear and minimal traction capacity telescoping becomes imminent. Wound-in-air also decreases the radial pressure in a wound roll which will decrease the torque capacity of the wound roll. This may well lead to internal slippage within the converting operation as the rolls are unwound. The effect of air entrainment in centerwound rolls has been studied by Good and Holmberg [1]. Bouquerel and Bourgin were the first to attempt to combine an elastohydrodynamic algorithm for the entrapped air with a wound roll model [2].

Thus it would seem worthwhile to be able to predict the effect of wound-in-air upon the wound roll structure. Such predictive tools become invaluable to investigate scenarios in which web speed may be increased or web line tension is decreased which seem to be the motifs in the production of webs today. Solution of this type problem is

two part. First, a model must be developed to predict the amount of air which is entrained into the winding roll and second, given the amount of entrapped air a second model must predict the impact upon the wound roll structure. In the case in which the air film can be predicted using a hydrodynamic solution the modeling discussed will be shown to be straightforward. If however the entrained air film must be modeled using elastohydrodynamic solutions the model for air entrapment cannot be separate from the model which computes the wound roll structure, since wound roll and nip deformations will be affecting the entrained air.

MODELS FOR THE ENTRAPPED AIR

A nip or rider roll in contact with the outer layers of a winding roll is an efficient means of controlling the amount of air which is entrained. To prove this point first consider the case of centerwinding with no rider roll as shown in Figure 1. Knox and Sweeney [3] established the height of an air film which exists between a web and an idler roller could be predicted by air foil bearing theory which had been presented by Blok and van Rossum [4]. Good and Holmberg [1] established that this same expression was valid for the condition of centerwinding without a rider roll. The expression for the air film thickness was:

$$h_{o,cw} = 0.65\, s \left[\frac{12\eta V}{T}\right]^{2/3} \tag{1}$$

Bertrum and Eschel developed a hydrodynamic expression which related the nip load to the air film thickness between a nip and a wound roll as shown in Figure 2 [5]. Their expression was:

$$L = 4\,\eta\, V \frac{r_e}{h_o} + \frac{4}{3\pi} \frac{T\sqrt{2\, r_e\, h_o}}{s} \tag{2}$$

The second term on the right hand side of expression (2) is negligible when compared to the first term. Thus expression (2) can be rearranged to provide an explicit expression for ho:

$$h_{o,nip} \approx \frac{4\,\eta\, V\, r_e}{L} = \frac{4\,\eta\, V\, s\, r_{nip}}{L\left(r_{nip} + s\right)} \tag{3}$$

Now a ratio of a centerwinding air film thickness to a centerwinding air film thickness with a nip can be expressed as:

$$\frac{h_{o,cw}}{h_{o,nip}} = .85 \frac{L}{(\eta V)^{1/3} T^{2/3}} \frac{\left(r_{nip} + r_s\right)}{r_{nip}} \tag{4}$$

Typical bounds for the nip load, L, and the web tension, T, range from 40 to 900 N/m. If the web velocity, radius of the nip, and the radius of the wound roll are chosen as 300 m/min, 0.1 m, and 0.5 m respectively, this ratio can range from 212 to 8680. Thus a nip or rider roll is a very effective means of reducing the amount of air which is entrapped by a winding roll.

Bouquerel and Bourgin [2] employed a elastohydrodynamic algorithm developed by Hamrock and Dowson [4]. To determine the lubricating film height in elastohydrodynamic problem requires the solution of both Reynolds' and elasticity equations. Hamrock and Dowson solved these equations over a wide domain of non-

dimensionalized parameters which involve load, velocity, and material factors which were appropriate for roller bearings lubricated by oils and grease. The following relation was developed specifically for materials of low elastic modulus:

$$h_{o,nip} = 7.43 R_x \left(1 - 0.85 e^{-0.31k}\right) U^{0.65} W^{-0.21} \tag{5}$$

Hamrock and Dowson's analysis assumed elliptical contact. It is inferred in their work that rectangular contact problems can be addressed with expression (5) if the parameter k is set greater than or equal to 10. In such a case the term within parentheses approaches unity and expression (5) becomes:

$$h_{o,nip} = 7.43 R_x U^{0.65} W^{-0.21} \tag{6}$$

One of the complexities in the application of an elastohydrodynamic algorithm to winding rolls is that the nondimensional speed and load factors, U and W, in expression (6) are functions of an effective modulus, E'. This is a combined modulus of the wound roll and the rider roll. The difficulty is that the radial modulus of the wound roll is dependent upon the interlayer pressure between the layers of web material which has been documented by several authors [6,7]. Polynomials in pressure have been used to represent the radial modulus of the wound roll as:

$$E_r = a + b\sigma_r + c\sigma_r^2 + c\sigma_r^3 \tag{7}$$

Typically in contact problems one first calculates the half width of contact followed by calculations of the pressures of contact. The Hertzian expression for the half width of contact for two cylinders in contact is:

$$b = \sqrt{\frac{2L}{\pi} \frac{\left[\left(1-\mu_{nip}^2\right)/E_{nip}\right] + \left[\left(1-\mu_r^2\right)/E_r\right]}{1/d_{nip} + 1/d_r}} \tag{8}$$

where the maximum and average pressures in the contact zone are:

$$p_{max} = \frac{2L}{\pi b} \quad \text{and} \quad p_{avg} = \frac{\pi}{4} p_{max} \tag{9}$$

Therefore the half-width of contact is a function of the pressure of contact through the radial modulus of the wound roll, E_r. An iterative calculation of the half-width and the average pressure of contact must be employed. In the iterative scheme, it may first be assumed that the modulus of the wound roll is equal to that of the nip and a resulting half width and average pressure can be calculated from expressions (8) and (9). In the next iteration the average contact pressure from the first iteration can be substituted into expression (7) for E_r, and a new solution for the half width and average pressure can be calculated from expressions (8) and (9). Thus a new average contact pressure results which can be input to (7) and the iteration continues. A solution is quickly converged upon which yields an appropriate value of E_r which can be input to E' and thereby into U and W in expression (6).

Please note that expressions (3) and (6) are independent of the web line tension, T_w. Both (3) and (6) are functions of nip load such that the implication is that the nip load is independent of web line tension. This is true only when the angle of wrap of the web about the nip or rider roll is zero or 180 degrees. For angles of wrap greater or less than 180 degrees there will be a component of web tension which will effectively increase or decrease the nip load.

COMPARISON OF THE MODELS

For the purpose of comparing the hydrodynamic and the elastohydrodynamic expressions (3) and (6), respectively, the nip load was allowed to range from 100 to 400 N/m and the web speed from 150 to 600 m/min. A nip with a radius of 5 cm. and a modulus of 1720 kPa was chosen. The computations would be used to emulate a roll wound from ICI Type 442 polyester wound with an average radius of 7 cm. The material thickness was 12.2 μm and the width was 15.24 cm. The tangential modulus and the radial modulus of elasticity (as measured in a vacuum) are:

$$E_t = 4.134 \text{ GPa} \quad \text{and} \quad E_{r,stack} = 480\sigma_r \text{ KPa} \tag{10}$$

The Hydrodynamic Solution

The nominal air film heights which resulted from employing the hydrodynamic expression (3) are shown in Figure 3. To determine if the air film heights shown in Figure 3 are large or small they must be compared to the roughness of the two web surfaces in contact. The mean surface roughness of the polyester film was 6.93 nm and the root mean square roughness was 9.54 nm. From the statistics of contact of two rough surfaces with a Guassian distributions of peak heights it can be shown that the mean gap between the two surfaces just brought in to contact is [8]:

$$\delta = Ra + 3\sqrt{2}\sigma \tag{11}$$

Therefore an air film thickness of 47 nm should be adequate to prevent all contact between adjacent surfaces of the Type 442 film. Thus air film heights ranging from 13 to 211 nm per Figure 3 could in some cases be accommodated by the gap but in other cases be ample to separate the web surfaces.

The Elastohydrodynamic Solution

The nominal air film heights which resulted from the elastohydrodynamic expression (6) are shown in Figure 4. It should be noted that expression (6) yields much greater air film heights than the hydrodynamic expression (3). Now the air film heights range from 380 to 1200 nm which is certainly ample to keep the web surfaces from contacting. Calculations performed using expression (6) required the iterative solution for E' using the procedure previously applied. To justify the use of this method for determining E', experimental measurements of the peak and average pressures were performed using an array of force sensitive resistors[1]. The results are shown in Table 1 and are indicative that the iterative method works reasonably well over the designated range of nip loading.

Experimental Data

With as much disparity as there was between the hydrodynamic and the elastohydrodynamic solutions the question must arise as to which is correct or at least more correct. To measure the air film layer thickness during the winding operation is difficult if not impossible. Good and Holmberg [1] were able to do this during centerwinding experiments but only because their air film layer heights were in excess of 25 μm, which was large compared to the runout of the wound roll surface tested. The method used by Good and Holmberg is inadequate to study air layers even 1200 nm thick,

[1] TEKSCAN, Inc, Boston, MA

the largest air layer encountered from the elastohydrodynamic solution. A technique was devised to measure the residual air after winding was completed. Rolls were wound under known conditions, submerged under water, and then unwound in our wound roll "bubblerimeter," refer to Figure 5. As the rolls were unwound the air became buoyant and was collected by a inverted funnel filled with water. Although most of the air escaped just as the web separated from the outside of the unwinding roll, some air would stick the web surface and was wiped from the web surface with rubber blades and collected by the funnel. The funnel had a graduated cylinder in which the air collects and can be measured. In these experiments the amount of air in solution in the water was negligible. The water inside the graduated cylinder is subject to a slight vacuum. Calculations have shown that this vacuum is responsible for a 3% increase in the volume of air measured, thereby the experimental data collected with the bubblerimeter is decreased by 3% such that the data reported represents the amount of air collected at atmospheric pressure.

An average air film thickness is calculated by dividing the volume of air collected by the surface area of the web using:

$$h_{o,avg} = \frac{Volume_{measured} * 10^3}{1500 * 0.1524} \text{ nm} \qquad (12)$$

where the volume is measured in milliliters. The experimentally measured average air film heights are shown in Figure 6. The velocities and nip loads may seem to be odd values but are the result of units conversion. The hydrodynamic and elastohydrodynamic air film heights were calculated using expressions (3) and (6) for these velocities and nip loads. The absolute value of the difference of the experimental and theoretical values were then recorded as an error term and are presented in Figure 7. The error ranges from 98 to 274 nm for the hydrodynamic case and from 262 to 826 nm for the elastohydrodynamic case. Thus the hydrodynamic expression (3) provides a solution with the least error and will be used henceforth to predict the wound-in-air.

Hamrock and Dowson's expression (6) is the result of a curve fit of numerical solutions of the elastohydrodynamic problem which were obtained using various values of U and W, the non-dimensionalized velocity and load, respectively. Hamrock and Dowson allowed U to range from $5.14*10^{-9}$ to $5.14*10^{-8}$ and W to vary from $1.76*10^{-4}$ to $2.20*10^{-3}$. For the conditions tested in the laboratory U ranged from $3.98*10^{-10}$ to $1.68*10^{-9}$ and W ranged from $8.43*10^{-3}$ to $2.39*10^{-2}$. Thus Hamrock and Dowson's expression should not be expected to yield a reasonable result when the values of U and W associated with the winding tests do not lie within the domains of U and W which were used in producing expression (6).

THE EFFECT OF ENTRAINED AIR UPON ROLL STRUCTURE

The effect of entrained air upon the wound roll structure is predominantly on the radial modulus of the wound roll in centerwinding [1]. When centerwinding with an rider roll there are two important effects. One effect is a similar reduction in the radial modulus but the second effect concerns the wound-on-tension. It has been proven at lower velocities that the web line tension is complimented by a nip induced tension, the sum becoming the wound-on-tension which would be used as input to a wound roll model for predicting the internal stresses in the wound roll [9,10]. The nip induced tension is limited by the friction, μ, between the wound-on-layer and the web layer beneath per the expression:

$$W.O.T. = T_W + \frac{\mu L}{h} \tag{13}$$

In many cases the air film layer which is formed will cause the wound-on-layer to become airborne and in such circumstances the wound-on-tension will become the web line tension, T_W. Air escape or exhaust from the roll ends may cause a loss in the radial pressure and the circumferential stresses through time but the focus of the current work is to study the amount of entrained air and the internal stresses within the roll just after winding.

Good and Holmberg [1] proposed a relation for radial modulus which is reduced by the entrained air layer. Assuming that the trapped air can be modeled as an ideal gas and that this air is entrained and trapped under isothermal conditions, the pressure and volume of the trapped air is governed by Boyle's Law,

$$[Pv]_0 = [Pv]_1 \tag{14}$$

The pressure under the external layer using an equilibrium equation for thin wall pressure vessels,

$$P_{o,gage} = \frac{T}{s} \tag{15}$$

As the pressure rises during winding, the volume decreases, see Figure 8.

$$(P_o + P_{atm})h_o = (\sigma_r + P_o + P_{atm})(h_o - x) \tag{16}$$

Solving for x and dividing by the original air film thickness yields a pseudo expression for the radial strain of the trapped air layer,

$$\varepsilon_r = \frac{x}{h_o} = \frac{\sigma_r}{\sigma_r + P_o + P_{atm}} \tag{17}$$

Taking the derivative with respect to the radial pressure, and inverting,

$$E_{r,air} = \frac{(\sigma_r + P_o + P_{atm})^2}{P_o + P_{atm}} \tag{18}$$

When the air film thickness is insufficient to entirely separate the layers both the compression of asperities and the entrained air will occur. Each successive layer of web material and the corresponding entrained air film layer behave as radial springs in series as shown in Figure 9. For springs in series:

$$K_{eq} = \frac{1}{\frac{1}{K_{stack}} + \frac{1}{K_{air}}} \tag{19}$$

or, after substitution,

$$\frac{1}{\left(\frac{E_{r,eq}A}{h_o + h}\right)} = \frac{1}{\left(\frac{E_{r,stack}A}{h}\right)} + \frac{1}{\left(\frac{E_{r,air}A}{h_o}\right)} \tag{20}$$

Finally, solving for the equivalent radial modulus,

$$E_{r,eq} = \frac{h_o + h}{\left(\frac{h}{E_{r,stack}}\right) + \frac{h_o(P_o + P_{atm})}{(\sigma_r + P_o + P_{atm})^2}} \tag{21}$$

where $E_{r,stack}$ is measured using a material testing system.

The air layer thickness and the surface roughness of the film must be compared to determine which of the above expressions for E_r is applicable. Generally three cases will describe conditions found during winding:

1. When the air film thickness is less than the mean surface roughness of the film, asperities between adjacent web surfaces contact unimpeded. The air layer is not a factor and no modification of E_r is required. $E_{r,stack}$ would be used as input in the wound roll model.

2. When the air film thickness is less than the mean gap between adjacent web surfaces but greater than the mean surface roughness (i.e. $R_a \leq h_o \leq R_a + 3\sqrt{2}\sigma$), the asperities can contact but this contact is reduced by the air film. $E_{r,eq}$ in expression (21) should be used as input in the wound roll model.

3. When the air film thickness is greater than the mean gap between adjacent web surfaces (i.e. refer to (11)) no asperity contact occurs between adjacent web surfaces. $E_{r,air}$ in expression (18) should be used as input in the wound roll model.

Note that all of the expressions for air entrainment presented herein (i.e. expressions (1), (3), and (6)) are functions of the outside radius of the wound roll. Thus it is quite probable that Cases 1, 2, and 3 may each occur during the winding of a roll. During startup at small winding radii and low winding velocity Case 1 could occur. As the winding roll becomes larger and the winding velocity increases Case 2 may become predominate. Finally as the wound roll is accruing its largest diameter the transition may be made to Case 3. This transition may often be catastrophic and unexpected in that a roll of fine appearance may be wound up to a given radius. At yet larger winding radii the web may become airborne which often leads to telescoping.

Rolls of ICI 442 polyester were wound at 610 m/min, a nip load of 117 N/m and a web line stress, T_w, of 6.89 MPa. Referring to Figures 3 and 6 it can be seen that the web should be completely airborne at these winding operating parameters and Case 3 should apply. Thus as previously discussed the web line tension will be the wound-on-tension. Pull tabs were used to determine the radial pressure profile but were not inserted by hand at these speeds. Prior to each experiment a roll of polyester was rewound at low speed and pull tabs [11] were affixed to the web. Rolls instrumented in this fashion were then rewound at the designated velocity and nip load. Results of four such experiments are shown in Figure 10. A wound roll model for internal stresses first presented by Hakiel [7] was implemented using expression (10) to determine a theoretical result for the radial pressure shown. The agreement between the experiments and the theoretical result was outstanding at all locations except the core which was expected. As winding begins at the core tension is difficult to control accurately and velocity must increase from zero to the velocity associated with the test condition. The variability in tension causes a wide dispersion in the radial pressure at the core, which is evident in Figure 10. The velocity starting from zero results in a Case 1 and later a Case 2 condition in the evaluation of E_r which will yield higher values of E_r in the core region and thereby higher radial pressures than those predicted theoretically, which is evident in Figure 10 as well. Note as well that in Figure 10 the results of two additional winding tests are shown. The nip load was increased to 350 N/m keeping all other winder operating parameters identical. The results were identical to the previous results where the nip loading was 117 N/m. This could have been predicted as the air film heights shown in Figures 3 and 6 still suffice to keep

the web airborne resulting in determining E_r from expression (18). Since the web was airborne the web line tension was still the correct input for the wound-on-tension. Thus with E_r and the wound-on-tension unchanged the same radial pressure profile should be expected as from the earlier tests in which the nip load was 117 N/m.

DISCUSSION

It was calculated that 47 nm of air film thickness could be accommodated prior to a total separation of the web surfaces occurring. It is shown per Figure 6 that the least error is associated with the hydrodynamic model and ranges from 98 to 274 nm. Thus the model for the air film thickness has by no means the accuracy required to assess which expression (9, 18, or 21) for E_r should be used as input for the wound roll model. The fact that for every tested condition there was more air collected in the experiments than was predicted using the hydrodynamic expression (3), please compare Figures 3 and 6, is indicative that a elastohydrodynamic solution is more realistic. Hamrock and Dowson's expression (6) predicts too much air, presumably because their expression was a curve fit which was developed for ranges of the nondimensionalized velocity and load terms, U and W, which were quite different than those associated with the winding of air into polymer film rolls. Thus there is an unsatisfied need for an elastohydrodynamic expression similar to Hamrock and Dowson's developed for the ranges of U and W encountered in the winding of air into rolls.

A leading indicator that air entrapment has become a problem during winding is the occurrence of telescoping. Jones [12] presented data that supported a hypothesis that telescoping is more a function of web velocity and tension than of nip force. With his permission the data has been presented herein as Figure 11. The data points show at what levels of web tension and velocity telescoping begins to appear as a function of nip load. Jones commented that a model for the wound-on-tension of the form of expression (13) does not agree with the telescoping data he presents. As previously discussed this agrees with the findings of this work in that after the web has become airborne there is no longer an effect of nip loading upon the radial pressure profile in the winding. The argument could be made that once the first layer becomes airborne above the second layer that the effective coefficient of friction has become minimal and the wound-on-tension stress in (13) is dependent only on the web line stress. The nip acts only as a metering device in controlling the amount of air which was entrained. This is shown in the air film thickness plots presented in Figures 3, 4, and 6 and in the radial pressure profile presented in Figure 10. If the radial pressure profile is independent of nip loading then the propensity to resist telescoping is as well independent of nip loading since this resistance is based upon the layer-to-layer traction capacity in the outer layers of the winding roll. There is some benefit of the nip roll even at low nip pressures as shown in Jones' data and in the extreme in what is called "gap" winding in which a roller is held in close proximity but not in contact with a centerwinding roll such that there is no nip loading. In such cases telescoping is in many cases limited due to the guiding action of the roller upon the web just prior to entering the winding roll. Thus tractile forces between the idling roll and the web also act to resist telescoping in concert with the interlayer tractile forces within the winding roll.

CONCLUSIONS

The wound roll "bubblerimeter" has provided valuable insight with regard to how much air is entrapped in winding rolls. Although the device yields reasonable, consistent data it has yet to be compared to other means of collecting entrained air data such as on-line density measurements as employed by Bouquerel and Bourgin [2].

The analysis of the internal pressures within wound rolls as affected by entrained air just after winding has been shown to be possible by using existing wound roll models with modification of the radial modulus and use of the proper wound-on-tension for the centerwinding condition [1] and for the case of the rider roll presented herein.

ACKNOWLEDGEMENTS

This publication is a result of research which was funded by the Web Handling Research Center of Oklahoma State University. The authors would like to thank the sponsors of the WHRC for supporting this research. The sponsors include the National Science Foundation, the Noble Foundation, the State of Oklahoma and an industrial consortium of which includes AET Packaging Films, Aluminum Company of America, E.I.Dupont de Nemours & Co.(Inc.), Eastman Kodak Company, Fife Corporation, Heidelberg-Harris Corporation, Hoescht-Diafoil Corporation, Mead Central Research, Mobil Chemical Company, Norton Company, Polaroid Corporation, Proctor & Gamble, Reliance Electric Company, Rexham Corporation, Sonoco Products Company, 3M Company, Valmet-Appleton Inc., and Xerox Corporation.

This research would not have been possible without the donation of polyester film and the associated roughness properties given by ICI Americas for which the authors are grateful and would like to personally thank William Stamper and Dilwyn Jones.

REFERENCES

1. Good, J.K. and Holmberg, M.W., "The Effect of Air Entrainment in Centerwound Rolls," Proceedings of the Second International Conference on Web Handling, Web Handling Research Center, Stillwater, Oklahoma, June 6-9, 1993.

2. Bouquerel, F., and Bourgin, P., "Irreversible Reduction of Foil Tension Due to Aerodynamic Effects," Proceedings of the Second International Conference on Web Handling, Web Handling Research Center, Stillwater, Oklahoma, June 6-9, 1993.

3. Knox, K.L., and Sweeney, T.L., 1971, "Fluid Effects Associated with Web Handling," Industrial Engineering Chemical Process Design Development, Vol 10, No.2, pp. 201-205.

4. Blok, H., and van Rossum, J.J., 1953, "The Foil Bearing Departure in Hydrodynamic Lubrication," Lubrication Engineering, Vol.9, Dec., pp. 310-320.

5. Bertrum, N. and Eschel, A., "Recording Media Archival Attributes," RADC-TR-80-123, pp. 68-73, April 1980.

6. Pfeiffer, J.D., "Internal Stresses in a Wound Roll of Paper," Tappi Journal, Vol. 49, no. 8, pp. 342-347, 1966.

7. Hakiel, Z. "Nonlinear Model for Wound Roll Stress," Tappi Journal, Vol. 70, no. 5, pp. 113-117, 1987.

8. Good, J.K. and Xu, Y., "Computing Wound Roll Stresses based upon Web Surface Characteristics," Proceedings of the Second International Conference on Web Handling, Web Handling Research Center, Stillwater, Oklahoma, June 6-9, 1993.
9. Good, J.K. and Wu, Z., "The Mechanism of Nip Induced Tension in Wound Rolls," Journal of Applied Mechanics, Vol.60, No.4, December 1993.
10. Good, J.K., Wu, Z., and Fikes, M.W.R., "The Internal Stresses in Wound Rolls with the Presence of a Nip Roller," Journal of Applied Mechanics, Vol. 61, No.1, March 1994.
11. Monk, D.W., Lautner, W.K. and McMullen, J.F. "Internal Stresses Within Rolls of Cellophane," Tappi Journal , Vol. 58, no. 8,August 1975.
12. Jones, D.P., "Air Entrainment as a Mechanism for Low Traction on Rollers and Poor Stacking of Polyester Film Reels, and its Reduction," Applied Mechanics Division, ASME, AMD-Vol.149, Web Handling - 1992, pp.123-131.

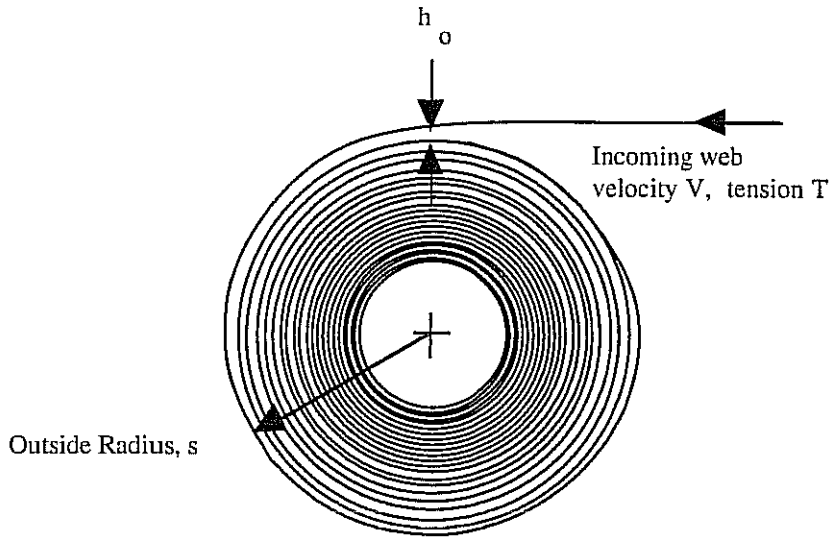

Figure 1 - Air Entrapment in Centerwinding

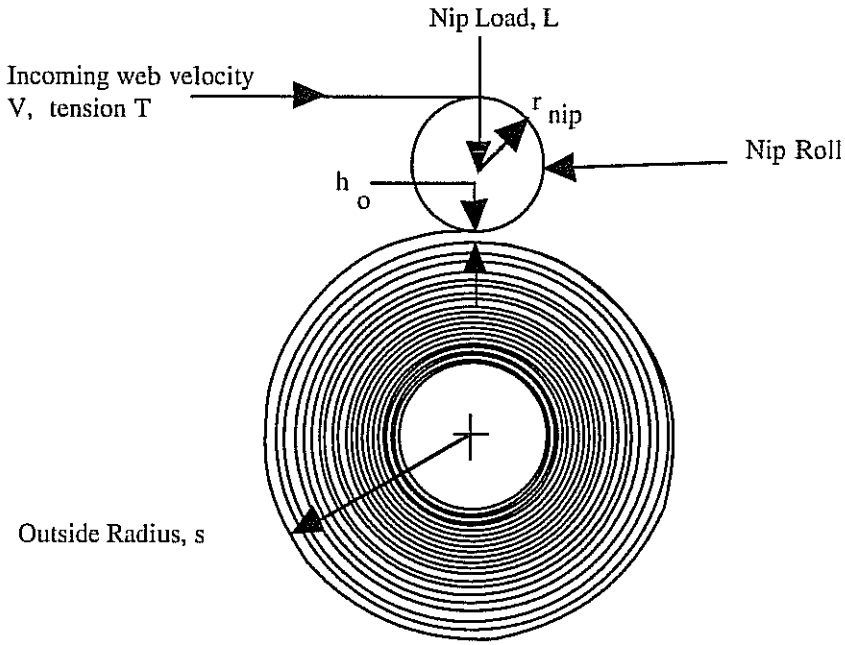

Figure 2 - Centerwinding with a Nip Roll

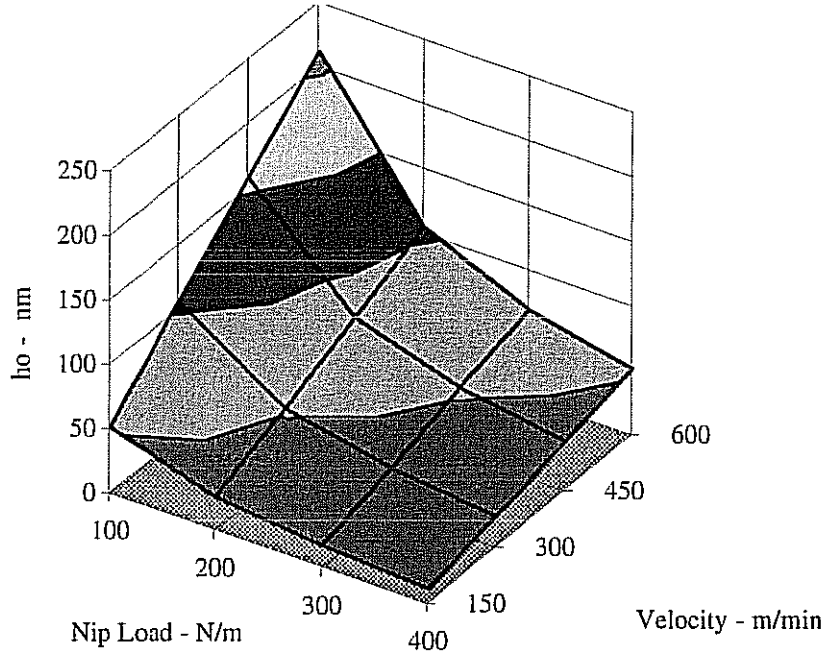

Figure 3 - Hydrodynamic Theory

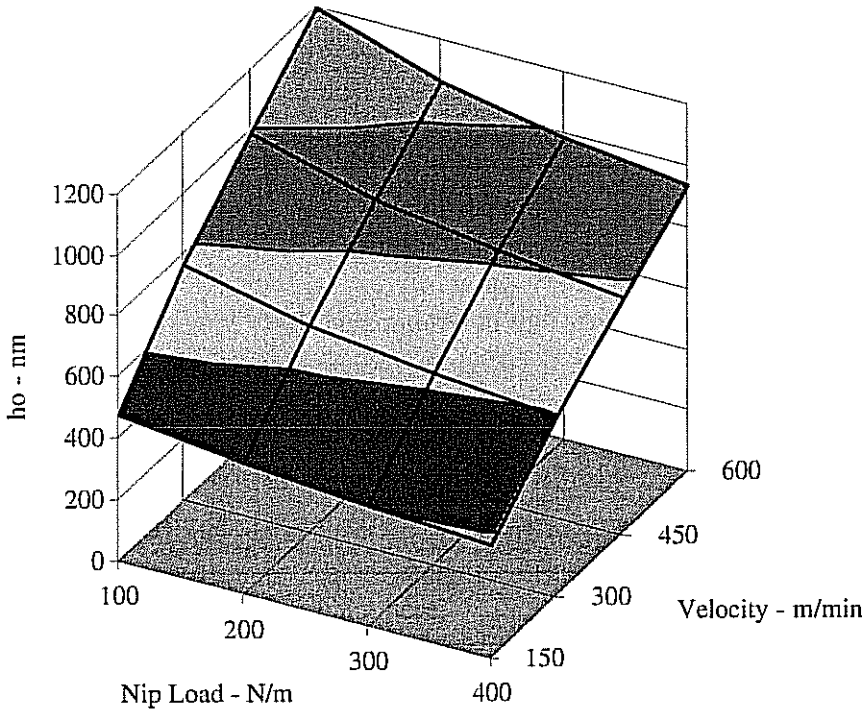

Figure 4 - Elastohydrodynamic Theory

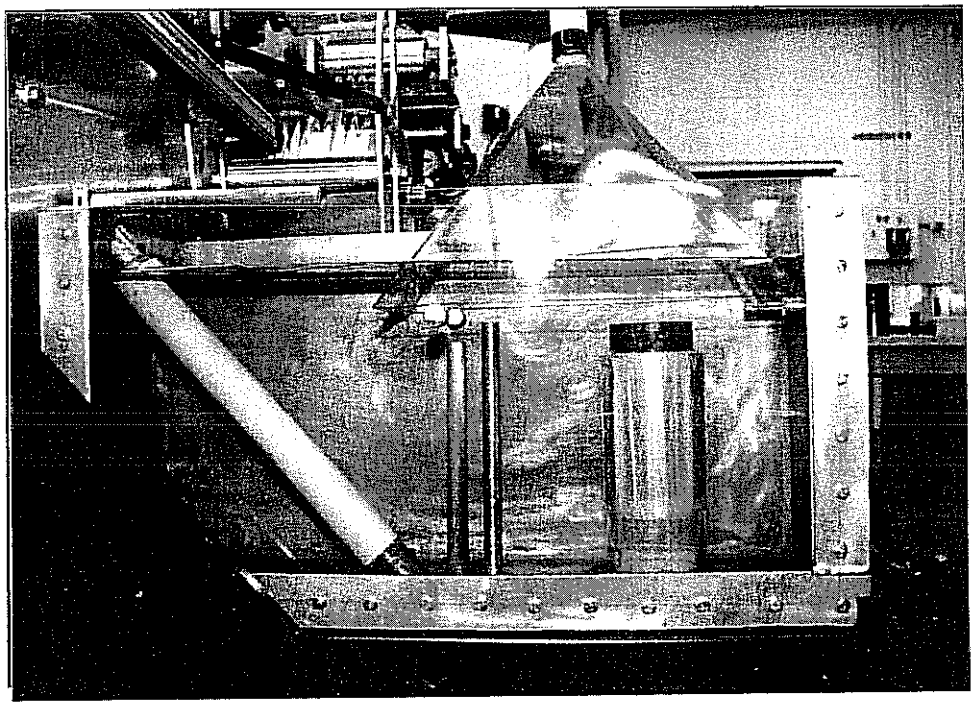

Figure 5 - The Wound Roll Bubblerimeter

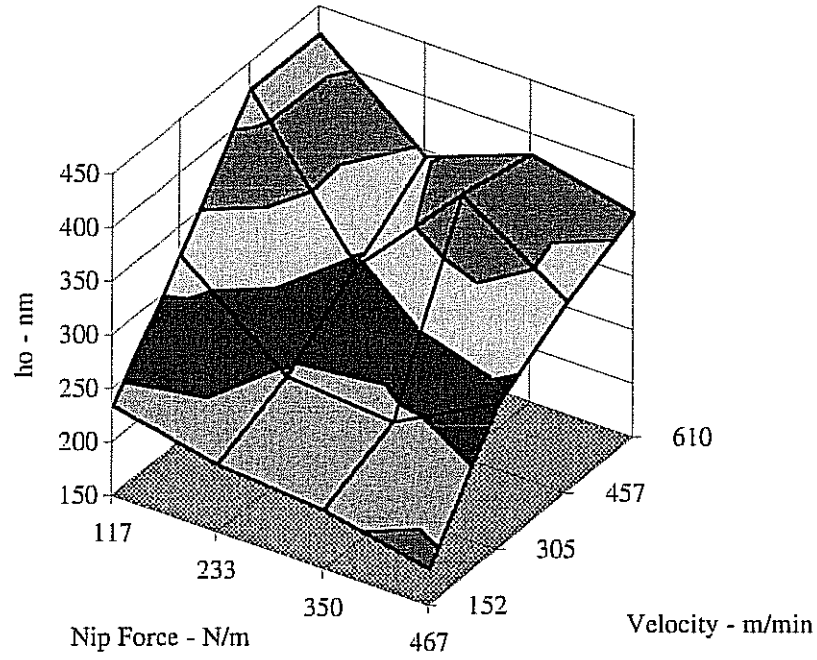

Figure 6 - Experimental Data

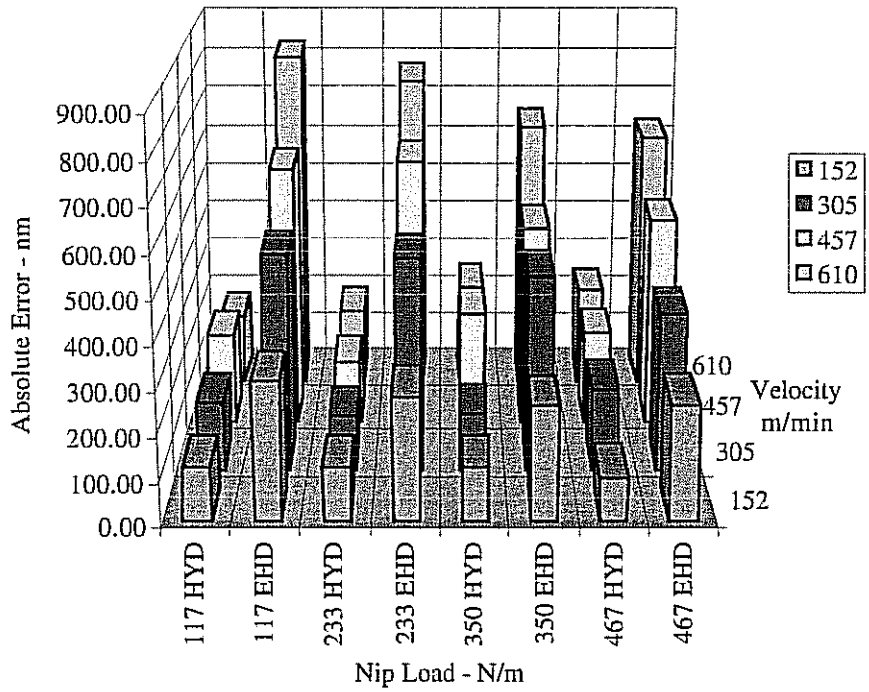

Figure 7 - Absolute Error, Experiments vs. Theory

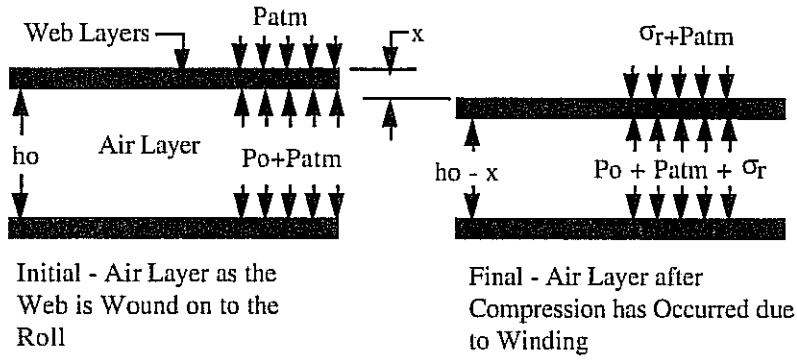

Figure 8 - The Compression of the Entrained Air due to Winding

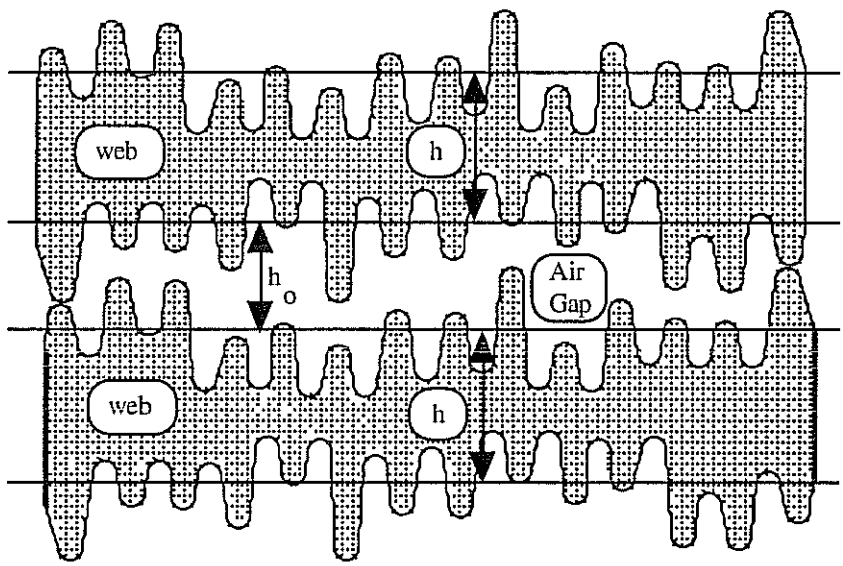

Figure 9 - The Compression of Asperities and Air

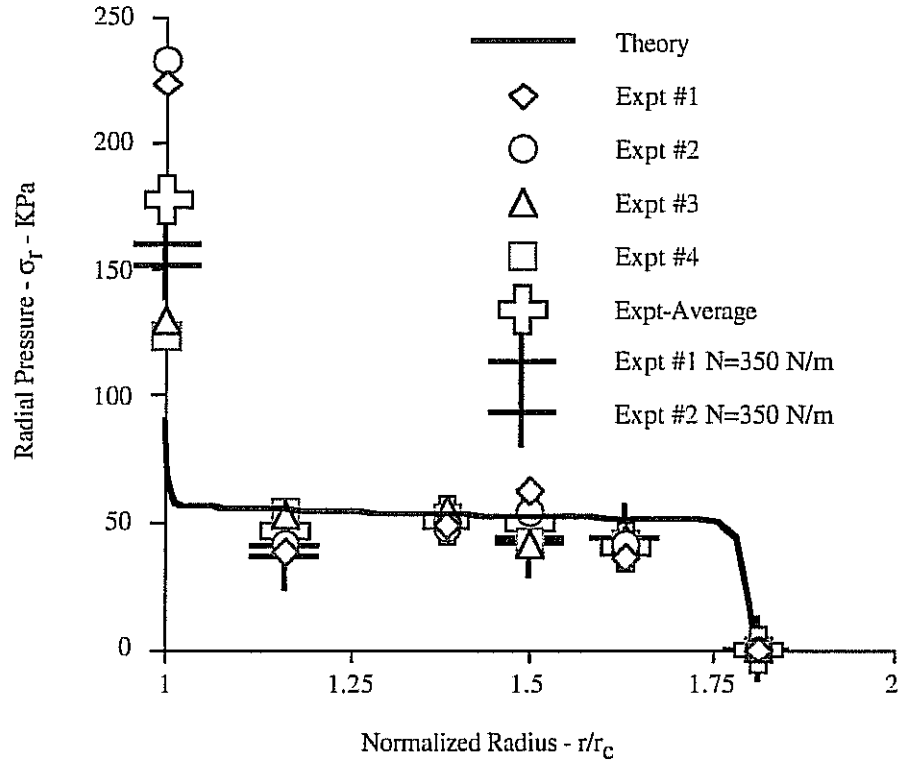

Figure 10 - Radial Pressure in Roll Wound at 610 m/min

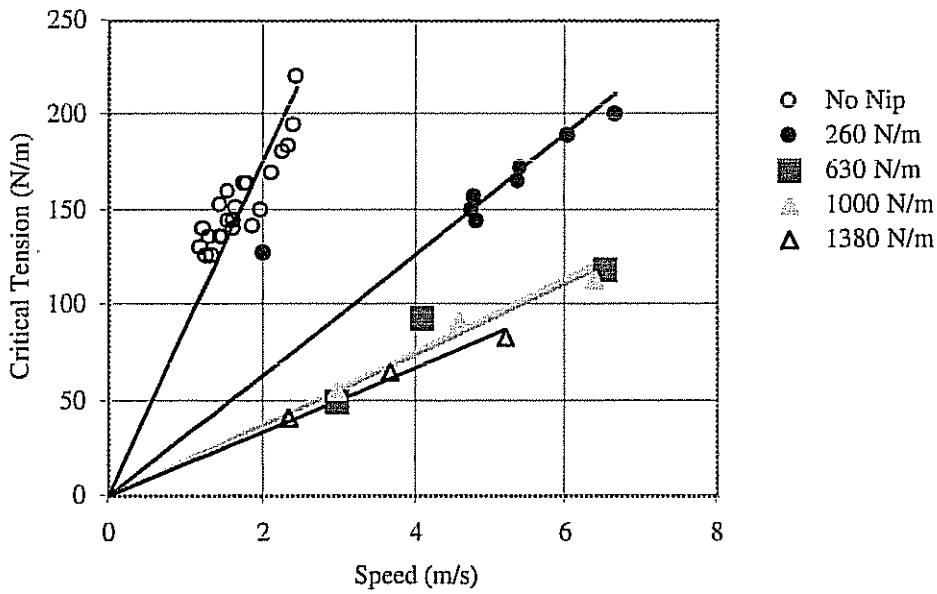

Figure 11 - Jones' Telescoping Data

Nip Load - N/m	Pressure - Peak Tested, KPa	Pressure - Average Tested, KPa	Er - based on Pavg,test	E' - based on Pavg,test, KPa
117	34.45	18.53	8896	3333
233	53.05	29.49	14155	3582
350	66.14	46.78	22456	3758
467	93.02	67.25	32278	3856

Nip Load - N/m	Pressure - Peak Iteration, KPa	Pressure - Average Iteration, KPa	Er - based on Pavg,iteration, KPa	E' - based on Pavg, iteration, KPa	%Error
117	48.24	37.88	18185	3686	10.58
233	69.29	54.42	26123	3803	6.15
350	85.46	67.12	32217	3856	2.60
467	99.09	77.82	37355	3888	0.82

Table 1 - Verification of Iteration Process to determine E'

ICI 442 Polyester film

T_w = 6.89 MPa

Nip Load = 117 N/m

Core - Steel

r_i = 3.81 cm

r_c = 5.08 cm

E_c = 63.2 GPa

Wound Roll

r_o = 9.2 cm

$E_{r,stack} = 129\,\sigma_r - .00537\,\sigma_r^2 + 8.426*10-6\,\sigma_r^3$ Kpa

$E_{r,stack}$(in vacuum) = $480\,\sigma_r$

$E_{r,air} = 102.5 + 2\sigma_r + \sigma_r^2/102.5$ KPa

E_t = 4.13 Gpa

Table 2 - Winding Parameters

Good, J.K.; Covell, S.M.
Air Entrapment and Residual Stresses in Rolls Wound with a Rider Roll
6/19/95 Session 2 1:35 - 2:00 p.m.

No questions.

Thank you.